

Polarization characteristics in polyelectrolyte thin film capacitors

Targeting field-effect transistors and sensors

Oscar Larsson

Norrköping 2009

Polarization characteristics in polyelectrolyte thin film capacitors

Targeting field-effect transistors and sensors

Oscar Larsson

Linköping Studies in Science and Technology. Licentiate Thesis No. 1412

Copyright © 2009 Oscar Larsson, unless otherwise noted

ISBN: 978-91-7393-535-7

ISSN: 0280-7971

Printed by LiU-Tryck, Linköping, Sweden 2009

Cover: Polarization in a polyelectrolyte capacitor

The positive ion migrates towards the negatively charged electrode while the negatively charged immobile polymer chain remains close to the positively charged electrode.

Abstract

Polymers are very attractive materials that can be tailored for specific needs and functionality. They can for instance be made electrically insulating or (semi)conducting, with specific mechanical properties. Polymers are often processable from a solution, which enables the use of low-cost manufacturing techniques to fabricate polymer devices. Polymer-based electronic and electrochemical devices and sensors have been developed.

This thesis is related to the polarization characteristics in polyelectrolyte thin film capacitor structures. The polarization characteristics have been analyzed at various humidity levels for polyelectrolyte capacitors alone and when incorporated as the gate-insulating material in polyelectrolyte-gated organic field-effect transistors. Both limitations and possibilities of this class of transistors have been identified. Also, a concept for wireless readout of a passively operated humidity sensor circuit is demonstrated. The sensing mechanism of this sensor is related to the polarization in a polyelectrolyte thin film capacitor. This sensor circuit can be manufactured entirely with common printing technologies of today and can be integrated into a low-cost passive sensor label.

Acknowledgements

Without the help and support from many people in my surrounding, I would not have reached this point. Here, I would like to express my gratitude to:

Xavier Crispin, my supervisor, and Magnus Berggren, my co-supervisor, for your help, encouragement, enthusiasm and for creating such an inspiring working environment.

Nate Robinson, my previous co-supervisor, for your support and that you always had time for my questions.

Sophie Lindesvik, for making everything related to administration so easy for me.

Brains and Bricks, for the financing of my research.

The entire Organic Electronics group, both previous and present group members, for your friendship, help and our interesting and stimulating (but not always science related) discussions.

David and PeO, for introducing me into the field of Organic Electronics and for your support since then.

Lars, for always having time for my questions and for giving me valuable comments on this thesis.

Klas, for the help related to mathematical modeling and all fun conversations (often related to sports).

Joakim, for the support and advices you still are giving me on my road towards a PhD, and for being a great friend.

My mother and father, Ewa and Göran, and my brother, Victor, for always being there.

Finally, the most important persons in my life: Anna, the love of my life, thank you for your never-ending support and for always believing in me. Oliver and Alva, all your energy and love makes me feel happy.

Papers included in this thesis

I:

Effects of the ionic currents in electrolyte-gated organic field-effect transistors

Elias Said, Oscar Larsson, Magnus Berggren and Xavier Crispin

Advanced Functional Materials **2008**, *18*, 3529-3536

Contribution: Part of experimental work. Wrote part of the first draft of the manuscript.

II:

Insulator polarization mechanisms in polyelectrolyte-gated organic field-effect transistors

Oscar Larsson, Elias Said, Magnus Berggren and Xavier Crispin

Advanced Functional Materials, In press, DOI: 10.1002/adfm.200900588

Contribution: All experimental and model-related work. Wrote the first draft of the manuscript and was involved in the final editing and submission of the manuscript.

III:

Proton motion in a polyelectrolyte: a probe for wireless humidity sensors

Oscar Larsson, Xiaodong Wang, Magnus Berggren and Xavier Crispin

Sensors and Actuators, B: Chemical, In press, DOI: 10.1016/j.snb.2009.09.043

Contribution: All experimental work and circuit design. Wrote the first draft of the manuscript and was involved in the final editing and submission of the manuscript.

Related work not included in this thesis

IV:

PEDOT:PSS-Based Electrochemical Transistors for Ion-to-Electron Transduction and Sensor Signal Amplification

M. Berggren, R. Forchheimer, J. Bobacka, P.-O. Svensson, D. Nilsson, O. Larsson and A. Ivaska

Book chapter in *Organic Semiconductors in Sensor Applications*, edited by D. A. Bernards, R. M. Owens and G. G. Malliaras, Springer, 2008.

V:

Moister sensor

Patent pending

VI:

Device for integrating and indicating a parameter over time

Patent pending

Table of contents

1. INTRODUCTION.....	1
2. MATERIALS	3
2.1. SEMICONDUCTING POLYMERS	3
2.1.1. <i>Molecular structure</i>	3
2.1.2. <i>Electronic charge carriers and charge transport</i>	6
2.2. POLYMER-BASED ELECTROLYTES.....	8
2.2.1. <i>Polymer electrolytes</i>	8
2.2.2. <i>Polyelectrolytes</i>	8
2.2.3. <i>Ionic charge transport</i>	9
3. IMPEDANCE SPECTROSCOPY	11
3.1. BASIC PRINCIPLES	11
3.2. COMMON EQUIVALENT CIRCUITS	15
3.2.1. <i>The Debye equivalent circuit</i>	15
3.2.2. <i>The Cole-Cole equivalent circuit</i>	16
3.2.3. <i>The Randles equivalent circuit</i>	16
4. POLARIZATION IN CAPACITOR STRUCTURES	19
4.1. POLARIZATION IN CAPACITORS BASED ON DIELECTRIC MATERIALS.....	19
4.2. POLARIZATION IN CAPACITORS BASED ON ELECTROLYTES	21
5. DEVICES.....	25
5.1. ORGANIC FIELD-EFFECT TRANSISTORS	25
5.1.1. <i>Device operation</i>	25
5.1.2. <i>Organic field-effect transistors operated at low voltages</i>	28
5.2. POLYMER-BASED HUMIDITY SENSORS	29
5.2.1. <i>Resistive- and capacitive-type sensors</i>	29
5.2.2. <i>Wireless readout and sensing of passive resonance sensor circuits</i>	30
6. CONCLUSIONS AND FUTURE OUTLOOK.....	35
REFERENCES.....	37

Background

1. Introduction

Polymers can be found in almost every product today due to the wide variety of properties of different polymers. Their mechanical and thermal properties can be tailored by modifying the building blocks, the monomers, and the bonding scheme of the polymers. They can, for instance, be made soft and flexible or hard and brittle. Further, polymers can be processed from a solution. Traditionally, polymers have been considered as electrically insulating materials and are, for instance, used as the insulating material around electrical conductors. This view of polymers, as electrically insulating, was changed with the discovery of conducting polymers in the late 1970s, by A.J. Heeger, A.G. MacDiarmid and H. Shirakawa for which they were awarded the Nobel Prize in Chemistry “*for the discovery and development of conductive polymers*” the year 2000 [1].

This discovery allows for materials that combine the mechanical properties and the processing advantages of polymers with the electrical and optical properties of metals or semiconductors [2]. As an example, semiconducting polymers can be processed from a solution. This ability enables the use of low-cost and high-volume manufacturing techniques, such as roll-to-roll printing, to produce electronic devices onto flexible substrates. This is in strong contrast to the expensive and complex manufacturing techniques that are used in the traditional semiconductor industry. Since the chemical and physical properties of polymers can be tailored for specific requirements, both conducting and non-conducting polymers have gained importance in the field of sensors [3]. Examples of polymer-based electronic devices that have been developed are light-emitting diodes [4, 5], solar cells [6] and field-effect transistors [7-9]. Polymer-based electrochemical devices include transistors [10] and logics [11], light-emitting electrochemical cells [12, 13] and display cells [14, 15], while examples of polymer-based sensors are humidity sensors [16, 17], biosensors [18] and ion-selective sensors [19, 20].

This licentiate thesis is related to polarization characteristics in polyelectrolyte thin film capacitors, with focus on their role in polymer-based field-effect transistors (Paper 1 and 2) and sensors (Paper 3). This first part of the thesis provides the background information necessary to understand the scientific results in the second part. The Background part serves as an introduction to the physical and chemical properties of polymer-based semiconductors and electrolytes (Chapter 2), material characterization with impedance spectroscopy (Chapter 3), polarization characteristics in polymer-based materials (Chapter 4) and device principles of polymer-based field-effect transistors and humidity sensors as well as to general resonance circuits (Chapter 5). At the end (Chapter 6), conclusions from the included papers are outlined together with a future outlook.

2. Materials

2.1. Semiconducting polymers

2.1.1. Molecular structure

Polymers are macromolecules that are built up from a large number of repeated units, monomers, connected through covalent bonds. In organic polymers the repeating unit(s) includes carbon atoms, which have the ability to bond with other carbon atoms to form chains. The electronic ground state configuration of an isolated carbon atom is $1s^2 2s^2 2p^2$. In the presence of atoms surrounding the carbon atom, the atomic orbitals of the valence electrons will be distorted and can instead be described with a set of hybrid orbitals. In a set of hybrid orbitals, each hybrid orbital has identical shape and energy but they are oriented in different directions.

The carbon atoms forming the skeleton of conventional polymers are sp^3 hybridized. The valence electrons of such a carbon atom are described with four hybrid orbitals, which can be found as linear combinations of the 2s and the three 2p atomic orbitals, forming a tetrahedral-shaped structure with an angle of about 109° between the hybrid orbitals. Each of the hybrid orbitals forms a single bond to a neighboring atom through σ -bonding. For a carbon atom in polyethylene, two of these four σ bonds are formed with adjacent carbon atoms while the remaining two σ bonds are formed with hydrogen atoms, see Figure 2.1a. The electrons involved in the σ bonds along the carbon backbone are strongly localized between the atoms that they hold together. This results in a large energy difference between the highest occupied molecular orbital (HOMO) and the lowest unoccupied molecular orbital (LUMO), in other words a large energy gap $E_g(\sigma)$, rendering these materials electrically insulating and transparent (Fig. 2.1b).

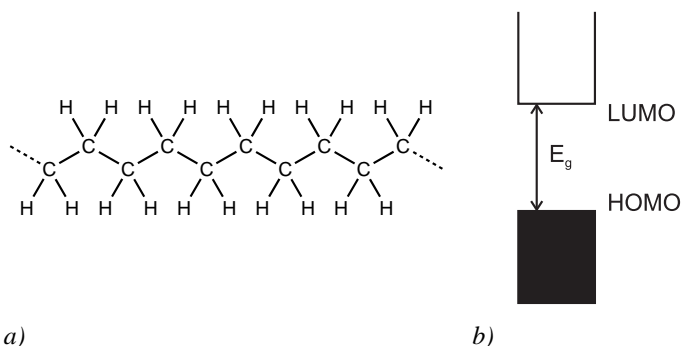


Figure 2.1. a) The molecular structure of polyethylene, and b) the large energy gap (E_g) between the HOMO and the LUMO.

In contrast to conventional insulating polymers each backbone carbon atom in a semiconducting polymer is sp^2 hybridized. For such a carbon atom, three of the four valence electrons are described with hybrid orbitals. These three hybrid orbitals, which can be found as linear combinations of the 2s and two of the three 2p atomic orbitals, forms a planar structure with an angle of 120° between the hybrid orbitals. The hybrid orbitals form σ bonds to neighboring atoms and create the backbone of the polymer. Like the electrons involved in the σ bonds along the carbon backbone of conventional polymers, the electrons involved in these σ bonds are strongly localized between the atoms that they hold together, leading to a large energy gap between the filled σ band and the empty σ^* band. The remaining valence electron, not participating in the sp^2 hybridization, is described with a 2p atomic orbital oriented perpendicular to the planar structure defined by the hybrid orbitals. When the 2p atomic orbitals of two adjacent carbon atoms overlap sideways they combine into two molecular orbitals, one π bonding molecular orbital and one π^* anti-bonding molecular orbital. Along the backbone of a semiconducting polymer chain that consists of N sp^2 hybridized carbon atoms (each contributes to a singly occupied 2p atomic orbital) there are a total of N 2p atomic orbitals that combine into N molecular orbitals with different discrete energy levels. In the electronic ground state, because each molecular orbital is capable of containing two spin-paired electrons, the $N/2$ lowest energy states, corresponding to the π bonding molecular orbitals, will be occupied leaving the higher energy π^* anti-bonding molecular orbitals empty.

For large values of N , as for polymers, the discrete energy levels become so closely spaced that they can be considered as a continuous energy band. If the π overlap of all adjacent 2p

atomic orbitals would be equal, meaning that the bonds between every carbon atom would have equal length, the π electrons would be completely delocalized along the backbone. The resulting energy band would then be half-filled and the polymer should behave as a one-dimensional metal. However, the energy of the system can be lowered by increasing the density of π electrons between every other carbon atom to create a π bond in addition to a σ bond, that is a double bond. By this introduction of alternating single and double bonds, or alternating long and short bonds, an energy gap is created, see Figure 2.2. This situation is described more generally by Peierls' theorem, which claims that a one-dimensional metal is always unstable with respect to a geometry modification that lowers the symmetry. The one-dimensional metallic structure of semiconducting polymers is thus not stable and undergoes a distortion, such as a bond alternation. As a result, a band gap $E_g(\pi)$ is opened up between the filled π band and the empty π^* band. The band gap of semiconducting polymers tends to be in the range 1.5-3 eV [21], which corresponds to the same range as inorganic semiconductors. With inorganic semiconductor terminology the completely filled π band is referred to as the valence band while the completely empty π^* band is referred to as the conduction band. In Figure 2.3 the molecular structures of different semiconducting polymers are displayed, note the pattern of alternating single and double bonds.

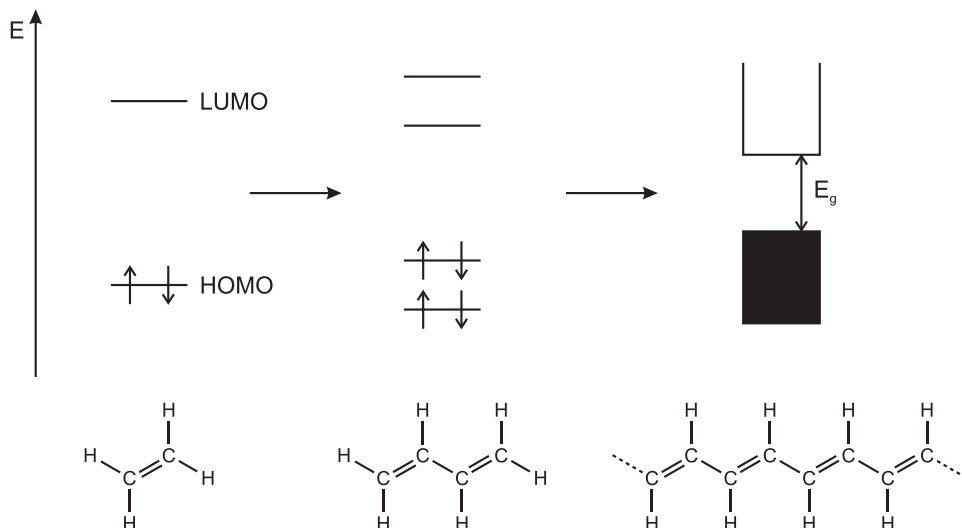


Figure 2.2. Electronic structures of molecules with sp^2 hybridized carbon atoms. The $2p$ atomic orbital of each carbon atom combines into molecular orbitals. For polymers (right), the discrete energy levels become so closely spaced that they can be considered as continuous energy bands.

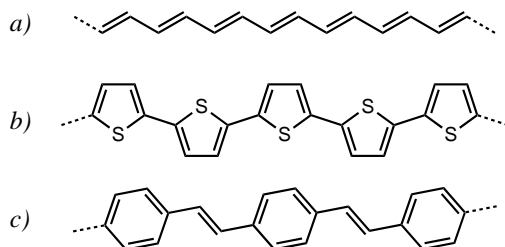


Figure 2.3. Molecular structures (short-hand notation) of three different semiconducting polymers. In a) polyacetylene, b) polythiophene, and c) polyphenylenevinylene.

2.1.2. Electronic charge carriers and charge transport

For a semiconducting polymer to be able to conduct electronic current, charge carriers must be introduced into the polymer. These charge carriers can be introduced via chemical or electrochemical doping, or via charge-injection. Most semiconducting polymers have a non-degenerate ground state with a preferred single and double bond alternation. The overall energy of non-degenerate ground state polymers depend on the bond alternation where the quinoid bonding configuration corresponds to a higher energy state compared to the aromatic bonding configuration. Charges (holes or electrons) introduced into such semiconducting polymers are stabilized by a local rearrangement of the bonding alternation in the vicinity of the charge. The charge together with the distortion of the bonding configuration is called a polaron and is delocalized over a small segment of the chain, see Figure 2.4. The formation of a polaron results in new localized states in the band gap. Polarons are singly charged, carry half-integral spin and can be either positive or negative.

Upon further addition of charges, polarons might combine. This result in two charges coupled to each other via a local rearrangement of the bonding alternation, this combination of charges coupled with the distortion of the bonding configuration is called a bipolaron. A bipolaron is doubly charged, carries no spin and can be either positive or negative. The formation of a bipolaron can be more favorable compared to the formation of two separate polarons; this is often the case in the presence of counter ions in the case of chemical or electrochemical doping. The localized states of a bipolaron are located further away from the band edges compared to the states of a polaron. The structures of a positive polaron and bipolaron are illustrated in Figure 2.4 together with their associated energy levels.

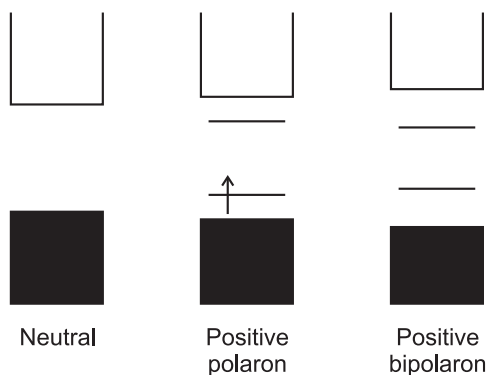
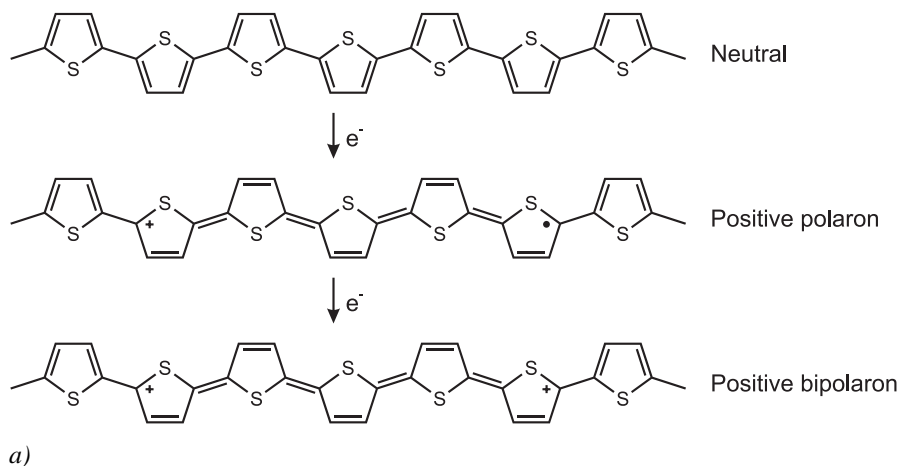


Figure 2.4. a) The structures of a neutral polymer chain, a positive polaron and a bipolaron, and b) their associated energy levels.

Due to weak π -overlap between neighboring polymer chains, charge carriers, in the form of polarons and/or bipolarons, tend to be delocalized on individual polymer chains [21]. A charge carrier on a specific polymer chain is transported along that chain as a package that alters the positions of the single and double bonds as it moves along the polymer backbone. This type of transport along specific polymer chains alone will however not yield conduction through an entire polymer sample since the polymer chains are of finite length and usually are disordered and contain defects. The conduction through an entire polymer sample is achieved via additional transport, in the form of hopping, of charge carriers between different polymer chains. This latter mechanism, hopping of charge carriers between polymer chains, limits the electronic charge transport.

2.2. Polymer-based electrolytes

Chemical compounds that are dissociated into free ions are called electrolytes. An electrolyte is an ionic conductor which may be in the form of a solution, a liquid or a solid [22]. Electrolyte solutions, consisting of a solute dissolved in a liquid solvent, are commonly suitable for electrochemical experiments. In such experiments, the choice of solvent is important since each solvent is associated with a stable potential window. However, from a practical point of view, ionically solid materials are often preferred instead of liquid materials in devices [23]. Primarily to avoid leakage-related problems and to allow for production of miniaturized structures with simple fabrication techniques. While some solid electrolyte systems are hard and brittle, which might cause contact problems at the electrolyte/electrode interfaces in devices without the use of liquid electrodes, the mechanical properties of polymer-based electrolytes allows for all-solid-state devices.

2.2.1. Polymer electrolytes

A polymer electrolyte, in its original sense, is referred to as a (liquid) solvent-free system in which an ionically conducting phase is created by dissolving salts in a high molecular weight polar polymer matrix [23]. For such dry polymer electrolytes, the solvent is the polymer itself. Both the positively (cations) and negatively (anions) charged ions can be mobile. Commonly, solvent-free polymer electrolytes are based on high molecular weight poly(ethylene oxide) (PEO, molecular structure in Figure 2.5a). PEO-based electrolytes have commonly a high degree of crystallinity at ambient temperatures. This results in a poor ionic conductivity in these electrolytes. One approach to achieve higher ionic conductivities relates to introducing small polar molecules into the polymer electrolyte. Such so called gel electrolytes are commonly referred to as polymer electrolytes but are created by dissolving a salt in a polar solvent and adding a polymer network to give the electrolyte mechanical stability.

2.2.2. Polyelectrolytes

Polyelectrolytes are materials that have a polymeric backbone with electrolytic groups covalently attached to it [23]. The electrolytic groups can be salts, acids and bases. Commonly, polyelectrolytes dissociate into ions in polar solvents. This results in charged polymer chains and oppositely charged counter ions. Depending on the chemical nature of the polyelectrolyte, the polymer chains become negatively or positively charged. A polymer chain that is negatively (positively) charged is called a polyanion (polycation). Since the polymer chains are immobile in the solid state, only one type of mobile ion exists in polyelectrolyte films. This is advantageous, for instance it makes the interpretation of conductivity

measurements much simpler than for polymer electrolytes. The molecular structures of a polyanion- and a polycation-based polyelectrolyte are given in Figure 2.5b and c, respectively.

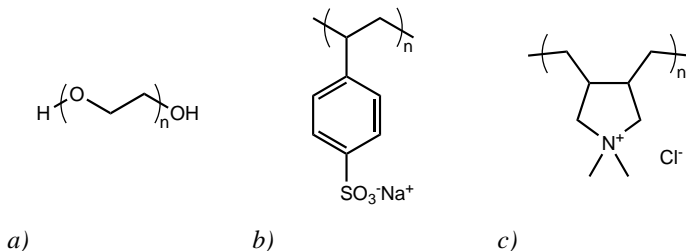


Figure 2.5. Molecular structures of a) poly(ethylene oxide) (PEO), b) poly(styrene sulfonate) with sodium as the mobile charge carrier (PSS:Na, polyanion-based polyelectrolyte), and c) poly(diallyldimethylammonium chloride) (polycation-based polyelectrolyte).

2.2.3. Ionic charge transport

The ionic transport mechanisms are dependent on the type of electrolyte. The major differences between the ionic motion in a polymer electrolyte and in a polyelectrolyte or a gel electrolyte are the molecular weight of the “solvent” and the interaction between the ions and the medium. In polymer electrolytes, the polymer matrix considered as the solvent for the ions have a high molecular weight. The polymer matrix, the solvent, is thus immobile and unable to participate in long-range motion. The ionic motion in polymer electrolytes takes place via sites that are created and destroyed on a continuous basis as a result of segmental motion of the polymer chains [23]. In a polyelectrolyte or in a gel electrolyte, on the other hand, low molecular weight solvents form a solvation shell around the ions. In these systems, the ions can move together with the solvent molecules belonging to the solvation shells. Since they are transported through the solvent they experience a frictional force related to the viscosity of the solvent, the size of the polymer network and the size of the solvated ions.

3. Impedance spectroscopy

3.1. Basic principles

Impedance spectroscopy is a powerful tool for the characterization of several of the electrical and electrochemical properties of a material and its interfaces with electrodes [24]. The material that is characterized can be in the solid or liquid states; and the method can investigate ionic, semiconducting or insulating (dielectric) properties. The sample is commonly situated inside a small measurement cell with metal electrodes at the ends, forming a sandwiched structure as illustrated in Figure 3.1. In the standard approach for impedance spectroscopy measurements, the impedance is measured by applying an alternating voltage with a specific frequency (f) to the measurement cell and measuring the amplitude and phase shift of the resulting current at f . This procedure is repeated for a number of frequencies within a specific frequency range, allowing the impedance to be measured as a function of frequency.

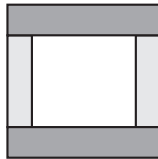


Figure 3.1. Cross-sectional illustration of a measurement cell. The material under test is located in the white center area, the top and bottom layer corresponds to the metal electrodes while the light grey walls hold the (liquid) material within the cell.

The frequency dependent complex impedance (Z) is defined in Equation 3.1 where ω is the angular frequency ($\omega = 2\pi f$), V is a complex voltage and I is a complex current.

$$Z(\omega) = \frac{V}{I} \quad (3.1)$$

Further, this impedance can be expressed as the sum of a frequency dependent real part (Z_{Re}) and a frequency dependent imaginary (Z_{Im}) part according to Equation 3.2 where j represents the imaginary number. The phase angle (θ) of the complex impedance is given in Equation 3.3.

$$Z(\omega) = Z_{\text{Re}} + jZ_{\text{Im}} \quad (3.2)$$

$$\theta(\omega) = \tan^{-1}\left(\frac{Z_{\text{Im}}}{Z_{\text{Re}}}\right) \quad (3.3)$$

With experimental data of the total complex impedance of a specific system in hand, either an electrical equivalent circuit or a mathematical model based on a physical theory is needed. Next, the experimental impedance data can be compared, or fitted, to the impedance expression of either the equivalent circuit or the mathematical model. It is only after that the information and parameters related to the electrical properties of the full system can be estimated. The parameters derived from an impedance spectroscopy measurement are generally grouped into two main categories:

1. Parameters that only are related to the material itself, examples are the dielectric constant and the conductivity of a material.
2. Parameters that are related to an electrode/material interface, examples are the capacitance of an interface region and parameters related to reactions at an interface.

Most of the electrical equivalent circuits contain ideal resistors and capacitors, while inductors rarely are included; the impedance expressions and phase angles of these circuit elements are summarized in Table 3.1. Usually, the resistors are used to describe irreversible processes such as interfacial charge transfer and charge transport, while the capacitors are used to describe reversible processes such as charge polarization or storage. The impedance response of four different equivalent circuits based on ideal resistors and capacitors are given in the form of Nyquist plots ($-Z_{\text{Im}}$ versus Z_{Re}) in Figure 3.2. Note that each point in a Nyquist plot corresponds to the impedance values at a specific frequency. The direction of the frequency is indicated with an arrow in the plots. The four different equivalent circuits in Figure 3.2 can,

for instance, be used to describe: a) an electric double layer, b) an electric double layer together with the resistance of an electrolyte, c) an electrochemical interface of a metal and an electrolyte where the resistor describes interfacial charge transfer and the capacitor describes the double layer at the interface, and d) an electrochemical interface as described in c) but with an additional resistor to account for the resistance of the electrolyte bulk. Thus, one way to obtain information or hints about a possible equivalent circuit of a specific system is to plot the experimental impedance data in a Nyquist plot and analyze its shape.

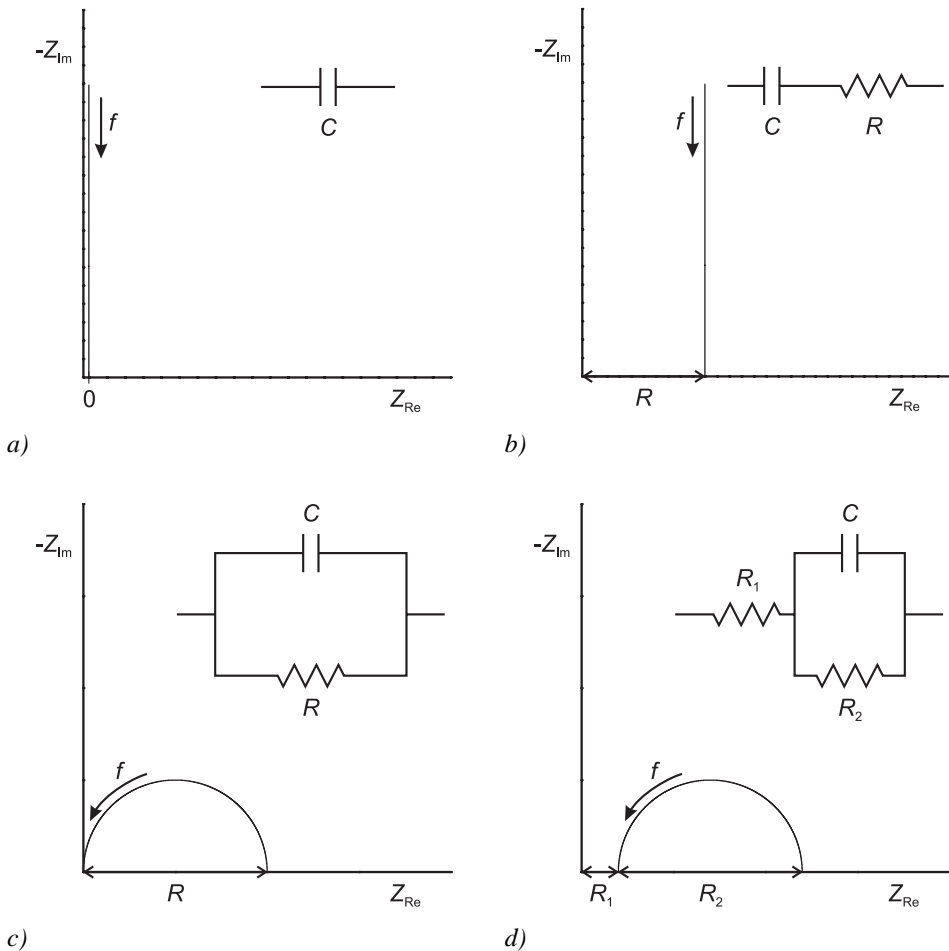


Figure 3.2. Four different equivalent circuits and their impedance responses presented as Nyquist plots. Note the direction of the frequency. From the plots, the values of the resistors can easily be obtained as indicated. The value of the capacitors can be calculated from the imaginary part of the impedances using the relation given in Table 3.1.

Circuit element	Impedance (Ω)	Phase angle ($^\circ$)
Resistor	$Z_R = R$	0
Capacitor	$Z_C = 1/(j\omega C)$	-90
Inductor	$Z_L = j\omega L$	90
Warburg impedance [25]	$Z_W = A/(j\omega)^{0.5}$	-45
Constant phase element [24]	$Z_{CPE} = 1/[Q_\alpha(j\omega)^\alpha]$	-90α ($0 \leq \alpha \leq 1$)

Table 3.1. The impedance expressions and the phase angles of the ideal circuit elements (resistor, capacitor and inductor) and the two most commonly used distributed circuit elements (the Warburg impedance and the Constant phase element).

However, impedance data of real world systems cannot always be described with equivalent circuits comprising only ideal circuit elements. This originates from the assumption that the time it takes for an electronic signal to travel between the circuit elements in a circuit is negligible. That is equivalent to considering the entire circuit to be located at a single point in space. However, in reality all systems are extended over a finite region of space, they are said to be distributed in space, rather than being localized at a single point. In addition, their microscopic properties might be distributed as well. Often, experimental impedance data exhibit a distributed behavior. In those cases, so called distributed circuit elements needs to be incorporated into the equivalent circuit to be able to approximate the experimental impedance with an equivalent circuit. The impedance of a distributed circuit element cannot be expressed exactly with a finite number of ideal circuit elements. Two of the most frequently used distributed circuit elements are the Warburg impedance and the constant phase element (CPE).

First; the Warburg impedance and its related phase angle are given in Table 3.1 where A is a positive constant [25]. This impedance element is related to mass transfer resistance and is specifically derived for (one-dimensional) diffusion of a particle [26]. From experimental impedance data, it is possible to estimate diffusion coefficients via the constant A . The Warburg impedance is frequently used within electrochemistry. Second; the CPE is an empirical impedance function with its impedance and phase angle given in Table 3.1 [24]. Q_α is a positive constant with its dimension altering with α , where α is a constant in the range $0 \leq \alpha \leq 1$. Note that: $\alpha = 0$ reveals the case of an ideal resistor with $R = Q_\alpha^{-1}$, $\alpha = 0.5$ gives the Warburg impedance with the constant $A = Q_\alpha^{-1}$, and that $\alpha = 1$ corresponds to the case of an

ideal capacitor with $C = Q_a$. CPEs are, for instance, frequently used in equivalent circuits to describe impedance data of solid and liquid electrolytes. In the literature, numerous different equivalent circuit models exist [24, 27]. Here, a few but general equivalent circuits are presented and described briefly.

3.2. Common equivalent circuits

3.2.1. The Debye equivalent circuit

The nominal time scale on which molecular reorientation or ion jumps can occur is called the relaxation time (τ) [28]. The basic model of dielectric relaxation is described with the Debye equivalent circuit [24, 29], see Figure 3.3a. The impedance response of this circuit is presented in a Nyquist plot in Figure 3.3b. This model is derived for materials with an absence of conductivity under the assumption of a single relaxation time. In the equivalent circuit, C_1 represents polarization established even at high frequencies of the applied field, while C_2 represents polarization established at low frequencies only. R represents the mechanism which acts to prevent the low frequency polarization from being established at higher frequencies. The single relaxation time in this model is given by $\tau = RC_2$. However, dielectric relaxation in many dielectric materials does not follow the Debye model with accuracy.

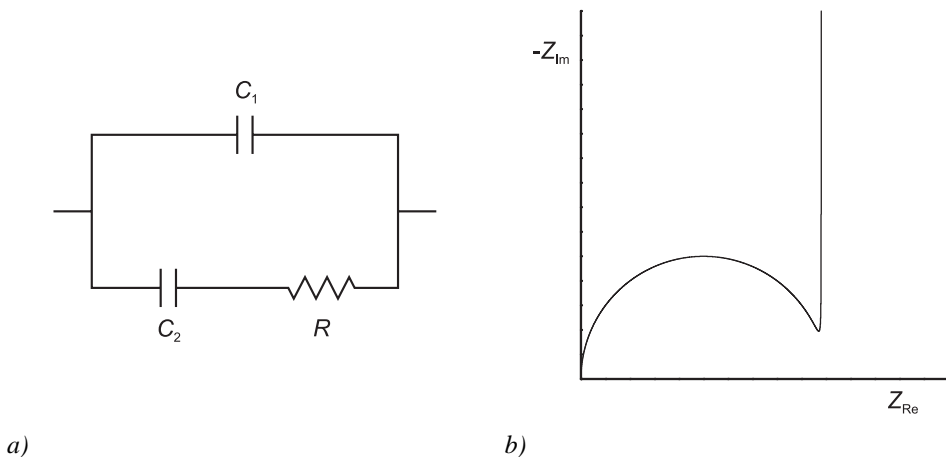


Figure 3.3. a) The Debye equivalent circuit, and b) its impedance response presented in a Nyquist plot.

3.2.2. The Cole-Cole equivalent circuit

The Cole-Cole model [29], described with the equivalent circuit in Figure 3.4a, of dielectric relaxation is derived for materials with an absence of conductivity and with a distribution of relaxation times [24]. In this model, this distribution is symmetric around a central relaxation time. The interpretation of the circuit elements in this equivalent circuit is identical to that of the Debye equivalent circuit with one exception; the mechanism which acts to prevent the low frequency polarization from being established at higher frequencies is represented by *CPE* in this circuit. Note that the Cole-Cole equivalent circuit will collapse into the Debye equivalent circuit if $\alpha = 0$. Thus, the distribution of relaxation times is related to the CPE and specifically to α ; a low (high) value of α corresponds to a narrow (wide) distribution. In Figure 3.4b, the impedance response of the Cole-Cole circuit is given for various values of α .

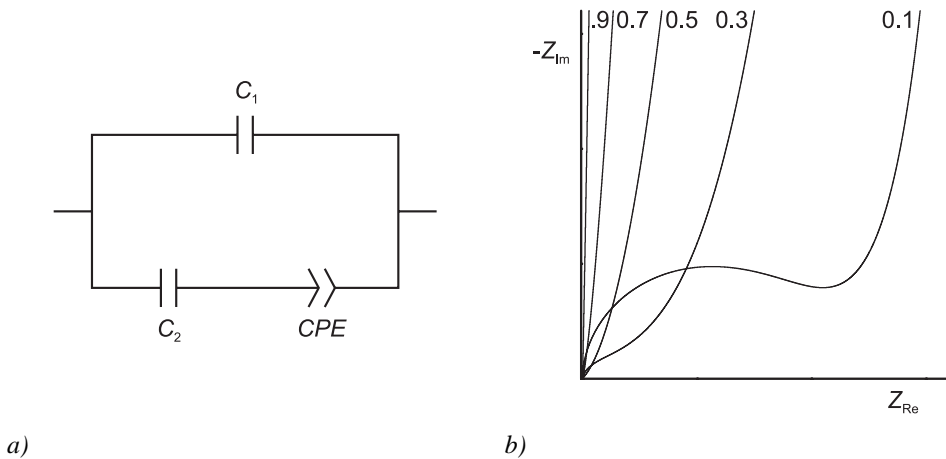


Figure 3.4. a) The Cole-Cole equivalent circuit, and b) its impedance response, for various values of α , presented in a Nyquist plot.

3.2.3. The Randles equivalent circuit

A frequently used equivalent circuit for electrochemical cells is the Randles equivalent circuit [22, 26]. This equivalent circuit is given in Figure 3.5a together with an illustration of an electrochemical half-cell (an electrode and an electrolyte). In this circuit, R_{CT} and C_{DL} are related to the electrolyte/electrode interface. R_{CT} represents interfacial charge transfer and C_{DL} represents the double layer formed at the interface. Further, Z_W is related to the diffusion layer. A slope of 45° at low frequencies of the impedance curve in the Nyquist plot (Fig. 3.5b)

is a characteristic of diffusion limitation at these frequencies. The last circuit element in this equivalent circuit, R_E , represents the electrolyte resistance.

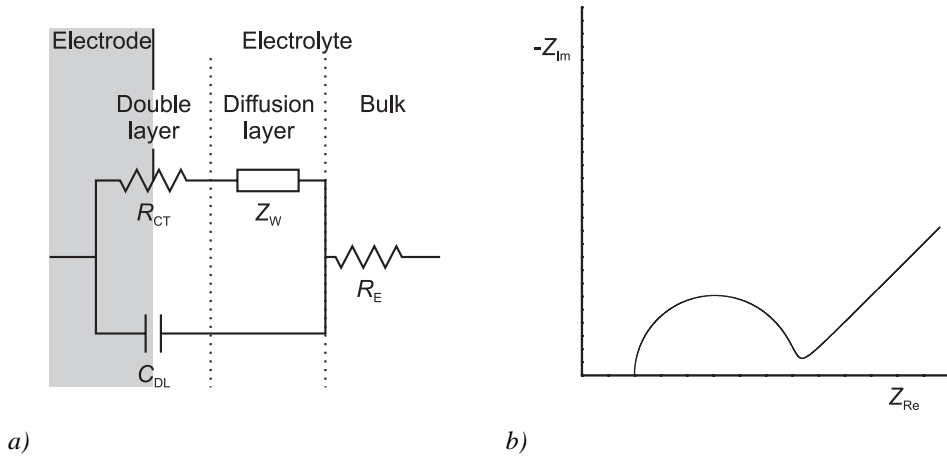


Figure 3.5. a) The Randles equivalent circuit together with an illustration of an electrochemical half-cell, and b) the impedance response of this circuit presented in a Nyquist plot. For details, see the text.

4. Polarization in capacitor structures

A capacitor consists of two electrical conductors separated from each other by an insulating material. The capacitance (C) between these two conductors is defined in Equation 4.1, where Q ($+Q$ on the positively biased side and $-Q$ on the grounded side) is the charge stored at or carried by each conductor and V is the potential difference between the two conductors.

$$C = \frac{Q}{V} \quad (4.1)$$

The charge polarization mechanisms and characteristics in capacitors are dependent on the character of the insulating material and the frequency of the applied field. Here, the polarization is described for capacitors with an organic dielectric material, and with an electrolyte, respectively, as the insulating material.

4.1. Polarization in capacitors based on dielectric materials

A dielectric material is a material that has no free charges that can move through the material under the influence of an electric field [30]. Since all electrons in a dielectric material are bound, the only possible motions in an electric field are very small displacements, in opposite directions, of positive and negative charges. A dielectric material in which this charge displacement has occurred is said to be polarized and its molecules are said to have induced dipole moments. The induced dipole moments are temporary and disappear when the electric field is removed. In addition, an electric field can also orient permanent dipole moments in the material. Here, the focus is on the orientation of permanent dipole moments in organic polymers. A solid state polymer sandwiched between two metal electrodes, forming a parallel-plate capacitor structure, is illustrated with dipoles in Figure 4.1a.

In a polymer, polar covalent bonds give rise to permanent dipole moments. These permanent dipole moments experience a torque that tends to align them with an applied electric field. In the solid state, the polar bonds tend to align, or rotate, with the electric field. This results in an equilibrium polarization with a net alignment of the permanent dipole moments with the applied field, idealized illustration given in Figure 4.1b. Additionally, the whole molecules themselves are capable to align with the electric field in the liquid state. The applied voltage between the metal electrodes results in a constant electric field (and linear potential profile) across the dielectric material. As the polarity of the applied voltage is reversed, the permanent dipole moments align with the new direction of the electric field (Fig. 4.1c). The polarity of the applied voltage can be modified with an ac voltage. Above a specific frequency of the applied ac voltage, the electric field changes direction faster than the permanent dipole moments can realign. As a result, the permanent dipole moments will not contribute to the polarization at these frequencies. This specific frequency is dependent on the strength of the molecular interaction with the material. It can be very high for a molecule in a fluid, and much lower in a solid [31, 32]. When the applied voltage is disconnected, the permanent dipole moments become randomly oriented and the polarization is lost (Fig. 4.1a).

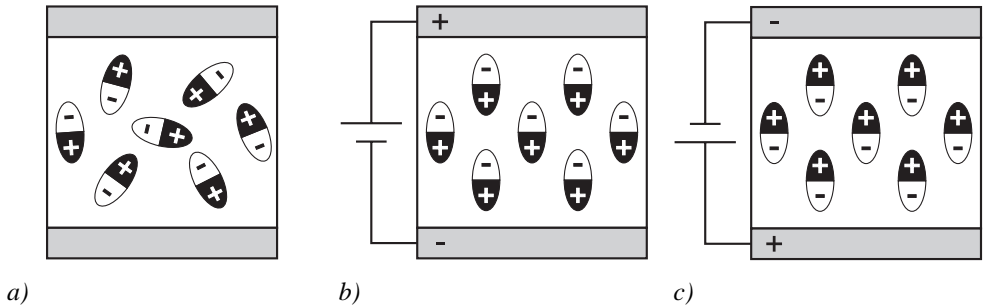


Figure 4.1. Idealized illustration of the polarization, due to the orientation of permanent dipole moments, in a capacitor (a dielectric polymer sandwiched between two metal electrodes). a) With no voltage applied, the permanent dipole moments are randomly oriented, b) with a voltage applied, the dipole moments align with the electric field, and c) when the polarity of the voltage is reversed, the dipole moments align with the new direction of the electric field.

The capacitance of a parallel-plate capacitor with a dielectric material as the insulating layer is given in Equation 4.2, where ϵ_0 is the permittivity of free space, κ is the relative dielectric constant of the dielectric material, A is the capacitor plate area and d is the thickness of the

dielectric material. A material with a large relative dielectric constant corresponds to a material that is polar or highly polarizable.

$$C = \frac{\epsilon_0 \kappa A}{d} \quad (4.2)$$

4.2. Polarization in capacitors based on electrolytes

In contrast to dielectric materials, electrolytes have free (ionic) charges that can move in an electric field. An illustration of a parallel-plate capacitor consisting of an electronically insulating but ion-conducting electrolyte sandwiched between two metal electrodes is given in Figure 4.2a. When a voltage is applied to the capacitor, redistribution of ions takes place in the electrolyte. Positively charged ions (cations) migrate towards the negatively charged electrode while negatively charged ions (anions) migrate towards the positively charged electrode (Fig. 4.2b). At the electrolyte/electrode interfaces so called electric double layers are formed (Fig. 4.2c).

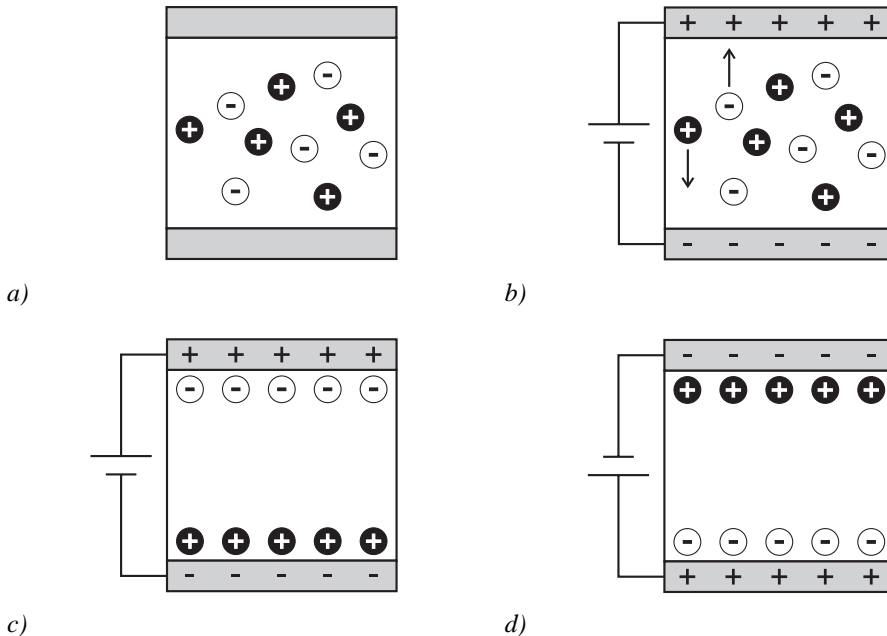


Figure 4.2. Idealized illustration of the polarization in a capacitor with an electrolyte sandwiched between the two metal electrodes. a) With no voltage applied, the ions in the electrolyte are randomly distributed. When a voltage is applied, b) ions migrate towards the oppositely charged electrode and c) forms electric double layers at the interfaces. In d), the polarity of the applied voltage is reversed.

Although electric double layers are formed at both interfaces, the focus will be on one of them here. The charge on the metal electrode (negative or positive dependent on the polarity of the applied voltage) is located in a very thin sheet ($< 0.1 \text{ \AA}$) on the surface of the metal [26]. The charge on the electrolyte side is made up of a surplus of ions (cations or anions dependent on the charge on the metal electrode) in the vicinity of the metal electrode surface. This ensemble of positive and negative charges, together with oriented dipole moments, at the electrolyte/metal electrode interface is called an electric double layer. Commonly, the structure of an electric double layer is described with the so called Gouy-Chapman-Stern (GCS) model [26, 31]. In the GCS model the electrolyte side consists of different layers, see illustration in Figure 4.3. Closest to the metal electrode is a layer that contains solvent molecules; this layer is called the compact layer or the Helmholtz layer. Next, a layer that consists of solvated ions a distance x from the metal electrode, that interact with the charged metal electrode via electrostatic forces. The potential profile from the metal electrode to x is linear; this region is represented by a capacitor C_H . The next layer is a diffuse layer that extends from x into the bulk of the electrolyte. In this layer there is an excess of ions that are oppositely charged compared to the metal electrode closest to the metal electrode. The potential profile in this layer decreases non-linearly towards the bulk of the electrolyte; this layer is represented by a capacitor C_D . The capacitance of the entire double layer, represented by C_H in series with C_D , is typically on the order of tens of $\mu\text{F}/\text{cm}^2$ [26]. Note that the electric field will be confined to the double layers. To compare with a dielectric capacitor, the capacitance of a 100 \AA thin SiO_2 layer is $\sim 0.35 \mu\text{F}/\text{cm}^2$ ($\kappa = 3.9$).

When the polarity of the voltage applied to the capacitor in Figure 4.2 is reversed, cations migrate towards the newly negatively charged electrode while anions migrate towards the newly positively charged electrode. Again, electric double layers are formed at the interfaces (Fig. 4.2d). An ac voltage can be used to cycle the polarity of the applied voltage. Now, if the frequency of the applied ac voltage is increased, a frequency is reached where the ions do not have enough time to form electric double layers. Above this frequency the ions migrate back and forth when the direction of the field is changed, they oscillate. When the applied voltage is disconnected, the ions become randomly distributed and the polarization is lost (Fig. 4.2a).

As with ordinary electrolytes, electric double layers will form at the interfaces when a polyelectrolyte is used as the insulating material sandwiched between the metal electrodes in Figure 4.2. However, since one of the charged species in a polyelectrolyte is practically

immobile (polyanion or polycation dependent on the polyelectrolyte) the formation of one of the electric double layers will be different. The positively (negatively) charged mobile ion will migrate towards the negatively (positively) charged electrode and form an electric double layer at that interface, while the double layer at the other interface is formed from the immobile polyanions (polycations) located close to the positively (negatively) charged electrode. At high frequencies, the mobile ions oscillate along the charged polymer chains.

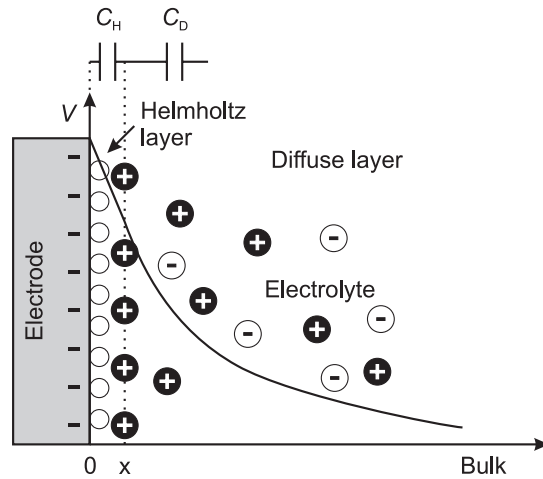


Figure 4.3. Illustration of the Gouy-Chapman-Stern model of the structure of an electric double layer. The empty circles represent solvent molecules and the black (white) circles with a '+' ('-') sign represent solvated cations (anions). See text for details.

5. Devices

5.1. Organic field-effect transistors

5.1.1. Device operation

The field-effect transistor (FET) is a three-electrode device (source, drain and gate) that is built up from electrically conducting, semiconducting and insulating materials. In an organic FET (OFET) the semiconducting layer is an organic material, for instance a semiconducting polymer. A schematic illustration of one electrode configuration is given in Figure 5.1, where L defines the channel length and W is the channel width.

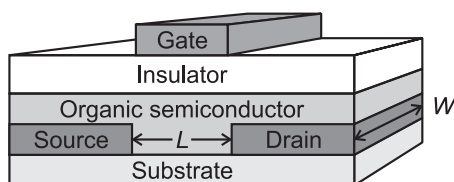


Figure 5.1. Schematic illustration of an organic field-effect transistor with channel length L and channel width W .

In FETs, the current through the transistor channel is controlled with a voltage applied to the gate electrode. OFETs operate in the accumulation mode in which an increase in gate voltage is associated with an enhanced conductivity of the transistor channel [33]. The gate electrode together with the gate-insulating layer and the organic semiconductor form a capacitor-like structure as illustrated in Figure 5.2a. Consequently, when a voltage is applied to the gate electrode, the gate insulator becomes polarized and charges are injected into the organic semiconductor from the source electrode, thus establishing the transistor channel, to charge the lower semiconducting capacitor-plate. For many OFETs, so called p -channel operation is most convenient [34]. For those transistors a negative voltage is applied to the gate electrode, followed by accumulation of positive (p) charge carriers in the transistor channel. The output

current of the transistor is driven by a voltage applied to the drain electrode. A change in gate voltage results in modulation of the charge carrier density in the transistor channel and thus a modulation of the output current of the transistor.

All of the accumulated charge carriers in the transistor channel are however not mobile, some of them are trapped in localized states at the semiconductor/insulator interface. When a voltage is applied to the gate electrode, these traps need to be filled before additional accumulated charge carriers can be mobile [34]. This means that mobile charge carriers in the transistor channel are obtained first when the applied gate voltage (V_G) is higher than a threshold voltage (V_T). Thus, below the threshold voltage ($V_G < V_T$) the transistor is off. For higher gate voltages ($V_G > V_T$), the evolution of the drain current (I_D) with increasing drain voltage (V_D) is described as follows (Fig. 5.2b-d):

- For low values of V_D the distribution of charge carriers is almost constant along the transistor channel, see Figure 5.2b. This results in a linear increase of I_D with increasing V_D . This regime is called the linear regime and the drain current ($I_{D, Lin}$) is given by Equation 5.1 where μ is the charge carrier mobility of the semiconductor and C_i is the capacitance per unit area of the gate insulator.

$$I_{D, Lin} = \frac{W}{L} \mu C_i (V_G - V_T) V_D \quad (5.1)$$

- At a higher value of V_D a point is reached where the charge carrier concentration in the transistor channel becomes zero close to the drain electrode, see Figure 5.2c. This point is called the pinch-off point and results in saturation of I_D ($I_D = I_{D, Sat}$ at $V_D = V_{D, Sat}$).
- As V_D is increased further ($V_D > V_{D, Sat}$) the pinch-off point moves further towards the source electrode, see Figure 5.2d. The potential at the pinch-off point ($V(x)$) remains constant ($V(x) = V_{D, Sat}$), resulting in a constant potential drop between the pinch-off point and the source electrode. As a result, the effective voltage applied to the channel will equal $V_{D, Sat}$ and I_D will remain constant ($I_D = I_{D, Sat}$). This regime corresponds to the saturated regime with the saturation current given by Equation 5.2.

$$I_{D,Sat} = \frac{W}{2L} \mu C_i (V_G - V_T)^2 \quad (5.2)$$

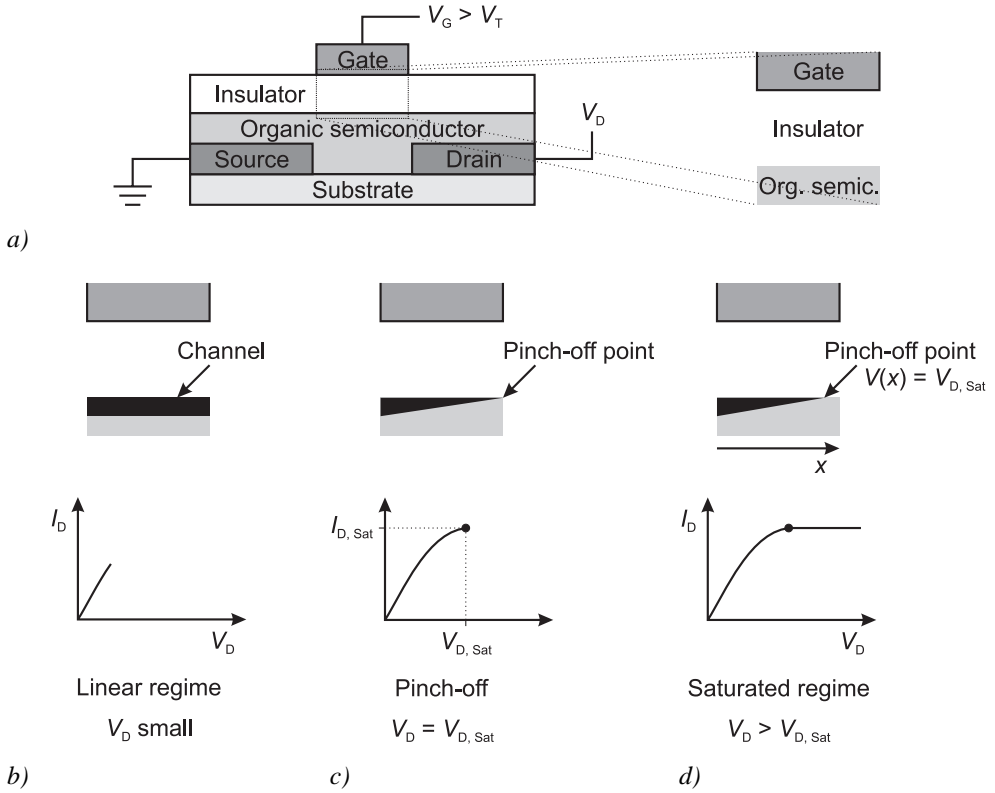


Figure 5.2. a) Schematic illustration of an organic field-effect transistor in which the capacitor-like structure, formed by the gate electrode, the insulator and the semiconductor, is zoomed-in. b-d) Illustrations of the operating regimes of the transistor with help of the zoomed-in structure in a) and corresponding current-voltage characteristics. b) The linear regime, c) pinch-off, and d) the saturated regime. See text for details.

For many electronic applications there is a demand for OFETs that can be switched on and off rapidly and that are capable of delivering high output currents at low driving voltages. Most often, the time response of an OFET is limited by the transit time (τ , Eq. 5.3 [35]) of the charge carriers through the transistor channel.

$$\tau \approx \frac{L^2}{\mu |V_D|} \quad (5.3)$$

From Equations 5.1-5.3 it is evident that a high charge carrier mobility of the semiconductor is essential to obtain high output currents and fast time response, at a given channel geometry, of OFETs. For this reason, much research has been devoted to find high-mobility organic semiconducting materials. Although the mobility is related to the nature of the semiconducting material, it is affected by several factors. It has been reported that good chain configuration (high regio-regularity) [36], a high molecular weight [37] and a high degree of crystallinity [38] of the polymer are key factors to achieve a high mobility. The degree of crystallinity is, in turn, dependent on the deposition method and can in some cases, for solution-processed polymers, be improved by the proper choice of solvent [38].

5.1.2. Organic field-effect transistors operated at low voltages

One major drawback with OFETs is that they in general require high operational voltages, often several tens of volts [33]. This excludes OFETs to be used in typical low-end applications where the available voltages are very low [39]. Currently, much attention is focused on lowering the operational voltages of OFETs. To simultaneously maintain as high output currents as possible, for a given charge carrier mobility of the semiconductor, the amount of accumulated charge carriers in the transistor channel should be as high as possible. At a specific gate voltage ($V_G > V_T$), without V_D applied, the accumulated mobile charge per unit area (Q_m) in the transistor channel is related to the gate voltage via Equation 5.4.

$$Q_m = C_i(V_G - V_T) \quad (5.4)$$

Clearly, a high capacitance per unit area of the gate insulator is required for low-voltage operation of OFETs, keeping the output current as high as possible (Eq. 5.1-5.2). The capacitance per unit area of a gate-insulating dielectric material is given in Equation 5.5, where ϵ_0 is the permittivity of free space, κ is the relative dielectric constant and d is the thickness of the dielectric layer.

$$C_i = \frac{\epsilon_0 \kappa}{d} \quad (5.5)$$

Hence, there are two different methods to increase the capacitance per unit area of a dielectric gate insulator: (i) change to a material with a large dielectric constant (high- κ materials) [40] or (ii) decrease the film thickness of the gate insulator [41, 42].

An alternative approach is to use an electrolyte as gate insulator instead of a dielectric material to achieve low operational voltages [43-49]. The device operation of an electrolyte-gated OFET is analogous to that of an ordinary dielectric-gated OFET, except for their differences in polarization of the gate insulator (a detailed description is given in Chapter 4). When a voltage is applied to the gate electrode of an electrolyte-gated OFET, electric double layers are formed along the two interfaces in contact with the electrolyte. These electric double layers are associated with a high capacitance per unit area, making low-voltage operation possible. One potential drawback with electrolyte-gated OFETs is that ions might penetrate into the organic semiconductor, resulting in electrochemical doping of the organic semiconductor bulk [50, 51]. In such case, the switching speed of the transistor is normally slow. Recently, *p*-channel OFETs gated via polyanion-based polyelectrolytes have been demonstrated [52, 53]. Electrochemical doping of the organic semiconductor in these transistors is prevented since the polyanions are immobile, meaning that they cannot penetrate into the semiconductor bulk. These transistors are operated at low voltages (< 1 V) with high output currents and exhibit fast turn-on and turn-off response (< 100 μ s) [54].

5.2. Polymer-based humidity sensors

5.2.1. Resistive- and capacitive-type sensors

Humidity sensors that are based on a change of the electrical impedance are commonly divided into two different groups; resistive- and capacitive-type sensors [55]. The resistive-type sensors are associated with a change of the real part of the impedance of the active sensing material with humidity, while the capacitive-type sensors are associated with a change of the imaginary part of the impedance. In the most common device configurations, regarding both resistive- and capacitive-type sensors, the humidity sensitive material is either sandwiched between two electrodes or deposited between interdigitated electrodes [56]. Among other materials, polyelectrolytes have been identified as good candidates for resistive-type humidity sensors due to their high sensitivity, quick response and low cost [57]. The molecular structure of a polyelectrolyte, poly(styrenesulfonic acid) (PSS:H), that is commonly used for resistive-type sensors is given in Figure 5.3a [56]. As water is absorbed into the polyelectrolyte film, the number of mobile counter-ions that are dissociated from the electrolytic groups of the polyelectrolyte, providing ionic current transport in the film, and the ionic mobility [58] of the polyelectrolyte change. Generally, the conductivity of polyelectrolytes increases nonlinearly with humidity [59, 60].

Although solid polyelectrolytes have been reported as a suitable class of material for capacitive-type sensors as well [61], the most common choice for capacitive-type sensors is to use an insulating polymer film as the active sensing material [56]. In Figure 5.3b, the molecular structure is given for an insulating polymer, poly(methyl methacrylate) (PMMA), that is commonly used for capacitive-type sensors [56]. Absorption of water into the insulating polymer film changes its dielectric constant, thus modulating its capacitance (Eq. 4.2). Due to the high dielectric constant of the absorbed water, the capacitance of these materials increases with humidity. Capacitive-type sensors are in general more expensive compared to resistive-type sensors, but they reveal more attractive characteristics on the other hand. Normally, they can be operated over a wider humidity range and exhibits a linear response with humidity, making the circuitry for interpretation of the humidity readout less complex [60].

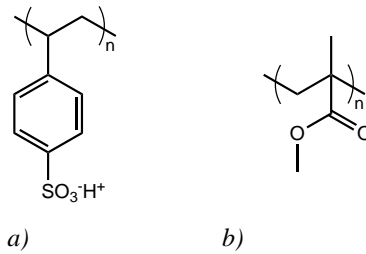


Figure 5.3. Molecular structures of a) poly(styrenesulfonic acid) (PSS:H), a commonly used polyelectrolyte for resistive-type humidity sensors, and b) poly(methyl methacrylate) (PMMA), a commonly used polymer for capacitive-type humidity sensors.

5.2.2. Wireless readout and sensing of passive resonance sensor circuits

A resonance circuit is an electrical circuit having an inductive and capacitive part. The simplest possible resonance circuit is a circuit that contains one inductor (L) and one capacitor (C). This type of resonance circuit is referred to as a LC circuit from here on. Such LC circuits can be configured in either a serial or parallel configuration (Fig. 5.4a and b). The total impedance of the serial (Z_{Serial}) and parallel (Z_{Parallel}) configurations are given by Equations 5.6-5.7.

$$Z_{\text{Serial}} = Z_L + Z_C = j\omega L - j\frac{1}{\omega C} = j\left(\omega L - \frac{1}{\omega C}\right) \quad (5.6)$$

$$Z_{\text{Parallel}} = \frac{Z_L Z_C}{Z_L + Z_C} = \frac{j\omega L \frac{-j}{\omega C}}{j\omega L - \frac{j}{\omega C}} = \frac{\frac{L}{C}}{j\left(\omega L - \frac{1}{\omega C}\right)} \quad (5.7)$$

At a specific frequency, called the resonance frequency (f_0), a large peak will be observed in the frequency response of each circuit's transfer function ($|V_{\text{Out}}/V_{\text{In}}|$ versus f , Fig. 5.4c). For the serial configuration, this peak will be observed at the frequency where the total impedance equals zero (Eq. 5.6), meaning that the LC circuit will act as an electrical short at f_0 . The resonance frequency of the parallel configuration will be observed where the impedance of the total impedance goes to infinity, in other words where the denominator equals zero (Eq. 5.7), meaning that the LC circuit will act as an open circuit at f_0 . The resonance frequency of a LC circuit, in either a serial or parallel configuration, is given by Equation 5.8. Note that additional reactive circuit elements added to a resonance circuit result in complex analytical expressions of its total impedance and resonance frequency.

$$f_0 = \frac{1}{2\pi\sqrt{LC}} \quad (5.8)$$

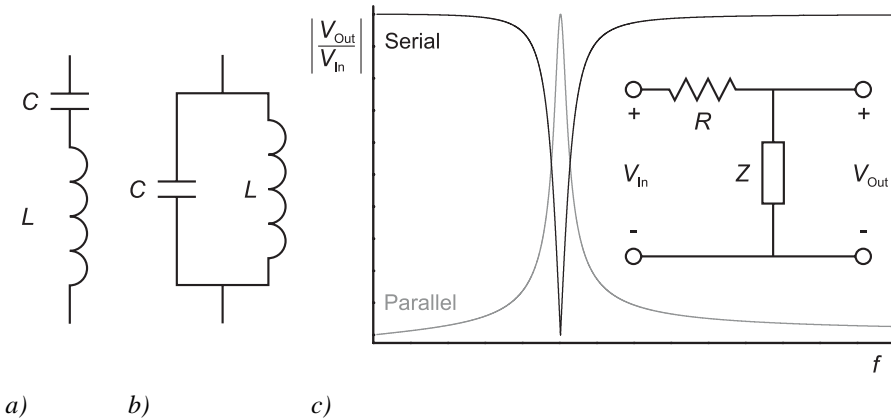


Figure 5.4. a) Serial and b) parallel configurations of LC circuits. c) The transfer functions of each LC circuit versus the frequency, Z corresponds to the circuits in a) and b). The frequencies at the peaks correspond to the resonance frequencies.

Now consider a circuit consisting of an ac voltage source connected to an inductor, called the primary side, separated from an unpowered LC circuit, called the secondary side, as illustrated in Figure 5.5a. The primary and secondary sides are mutually coupled within a certain physical distance. The current (I_P) through the inductor (L_P) of the primary side creates an alternating magnetic field that induces an alternating voltage ($V_{S, \text{Ind}}$) across the inductor (L_S) of the secondary side. $V_{S, \text{Ind}}$ drives an alternating current (I_S) through the secondary side. The current through L_S creates in turn an alternating magnetic field that induces an alternating voltage ($V_{P, \text{Ind}}$) across L_P , driving an alternating current through the primary side. The resulting circuit scheme of this mutual coupling is given in Figure 5.5b. If sinusoidal voltages and currents are assumed, the expressions for $V_{S, \text{Ind}}$ and $V_{P, \text{Ind}}$ are given in Equations 5.9-5.10, where M represents the mutual inductance between the primary and secondary sides.

$$V_{S, \text{Ind}} = j\omega MI_P \quad (5.9)$$

$$V_{P, \text{Ind}} = -j\omega MI_S \quad (5.10)$$

By applying Kirchhoff's voltage law on the primary and secondary sides, the following equations are obtained from the primary (Eq. 5.11) and secondary (Eq. 5.12) sides:

$$V_P = j\omega L_P I_P - j\omega MI_S \quad (5.11)$$

$$j\omega MI_P = I_S \left(j\omega L - \frac{j}{\omega C} \right) = I_S Z_S \quad (5.12)$$

where Z_S corresponds to the total impedance of the secondary side. Substitution of I_S (Eq. 5.12) into Equation 5.11 gives the total impedance of the primary side (Z_P) (Eq. 5.13). As shown in Equation 5.13, the total impedance of the secondary side is reflected to the primary side. The reflected impedance (Z_R) is given in Equation 5.14.

$$Z_P = \frac{V_P}{I_P} = j\omega L_P + \frac{\omega^2 M^2}{Z_S} \quad (5.13)$$

$$Z_R = \frac{\omega^2 M^2}{Z_S} \quad (5.14)$$

The impedance reflection implies that the impedance of the secondary side can be readout from the primary side without the need of a power source on the secondary side since all energy needed is transferred from the primary side. Thus, passive and wireless readout of the resonance frequency of a LC circuit is possible. This concept has been utilized by others to form LC circuits built up from capacitive-type humidity sensors together with an inductor, enabling wireless readout of the humidity level (Eq. 5.8) [62-64].

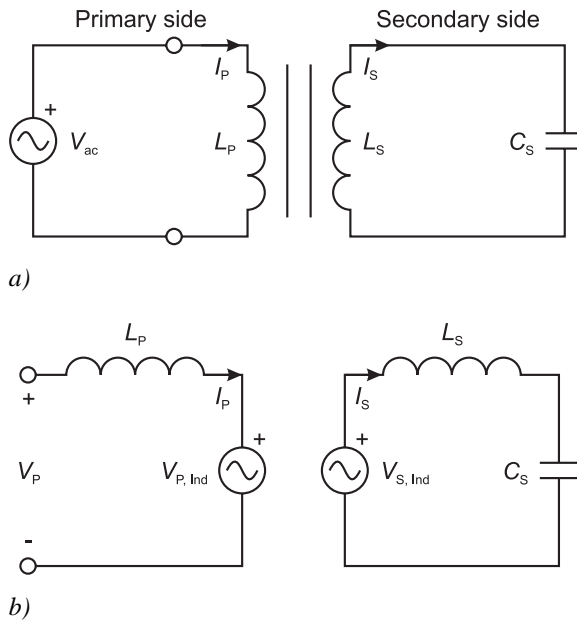


Figure 5.5. a) An ac voltage source connected to an inductor, forming the primary side, mutually coupled to a LC circuit that forms the secondary side. The circuits in b) represent the equivalent circuits of the mutual coupling. See text for details.

6. Conclusions and future outlook

This section aims to connect the results from the three papers that are included in this thesis and to present the major conclusions from each of them. More specific conclusions can be found at the end of each paper. Also, ongoing and prospective future works related to these papers are commented.

The common point for the three papers, despite the fact that two of them are related to OFETs (Paper 1 and 2) and one is related to sensors (Paper 3), is that they are related to the polarization of a polyelectrolyte in which the water content is varied. In Paper 2 it was found that the polarization characteristics in a polyelectrolyte capacitor could be divided into three different frequency regions between 100 Hz and 1 MHz. At high frequencies a region attributed to dipolar relaxation in the polyelectrolyte, at intermediate frequencies a region attributed to ionic relaxation; and at low frequencies, a region attributed to the formation of electric double layers at the polyelectrolyte/electrode interfaces. The transitions between the regimes of the different polarization mechanisms were shifted towards higher frequencies when the water content (proton conductivity) in the polyelectrolyte was increased.

In the same paper (Paper 2) it was found that the polarization of the polyelectrolyte limits the time response of polyelectrolyte-gated OFETs with short channel lengths. The three different polarization mechanisms of the polyelectrolyte explained the evolution of the saturation current versus time for those transistors between 200 μ s and 1 ms. Above 1 ms and for higher gate voltages, another phenomenon starts; the electrolysis of water. Paper 1 describes the impact of this electrochemical side reaction on the current-voltage characteristics of the OFETs. It was shown that a large part of the leakage current originated from the electrolysis. Hence, this class of OFETs should be operated in a dry environment. Surprisingly, even at low humidity levels, for which the ionic mobility is significantly decreased, the OFETs were still able to respond quickly to the gate voltage. The OFETs are expected to operate at even

higher frequencies if the ionic mobility of the electrolyte is high. This means that the ideal electrolyte for these transistors should be a solid electrolyte with high ionic mobility, even in dry environments. Recently, this class of transistors has been reported as promising candidates for the use in low-voltage printed electronic applications [65].

Further, in Paper 3, the ionic relaxation in a polyelectrolyte has been utilized as the sensing probe in a passively operated humidity sensor that was readout with a wireless technique. The sensor circuit is compatible with existing low-cost and high-volume manufacturing techniques, and can be integrated into a low-cost flexible electronic sensor label. This enables (humidity) sensing in new application areas that previously has been too expensive to monitor with existing sensor technologies. These sensors can, for instance, be permanently mounted inside walls or beneath floors in houses and buildings for wireless monitoring of eventual leakage or moisture problems. Also, drying processes inside materials and monitoring of the status of humidity sensitive goods during transportation and storage are possible applications. The polyelectrolyte used as the humidity sensitive material in these sensors is soluble in water, which limits the humidity range of practical use to lower humidity levels. However, this problem can be solved by different methods, for instance via copolymerization or cross-linking [66, 67]. On the other hand, a polyelectrolyte that becomes dissolved at high humidity levels gives the sensor a memory of that it has been exposed to a high humidity level. Ongoing and future work relates to fabricate the complete sensor circuit entirely with low-cost manufacturing techniques on one common flexible substrate or label.

References

- [1] *The Nobel Prize*, <http://nobelprize.org>, accessed September 2009
- [2] A. J. Heeger, *Journal of Physical Chemistry B* **2001**, *105*, 8475-8491.
- [3] B. Adhikari, S. Majumdar, *Progress in Polymer Science* **2004**, *29*, 699-766.
- [4] J. H. Burroughes, D. D. C. Bradley, A. R. Brown, R. N. Marks, K. Mackay, R. H. Friend, P. L. Burns, A. B. Holmes, *Nature* **1990**, *347*, 539-541.
- [5] M. Berggren, O. Inganäs, G. Gustafsson, J. Rasmussen, M. R. Andersson, T. Hjertberg, O. Wennerström, *Nature* **1994**, *372*, 444-446.
- [6] C. J. Brabec, N. S. Sariciftci, J. C. Hummelen, *Advanced Functional Materials* **2001**, *11*, 15-26.
- [7] A. Tsumura, H. Koezuka, T. Ando, *Applied Physics Letters* **1986**, *49*, 1210-1212.
- [8] G. Horowitz, *Advanced Materials* **1998**, *10*, 365-377.
- [9] H. Sirringhaus, *Advanced Materials* **2005**, *17*, 2411-2425.
- [10] D. Nilsson, M. Chen, T. Kugler, T. Remonen, M. Armgarth, M. Berggren, *Advanced Materials* **2002**, *14*, 51-54.
- [11] D. Nilsson, N. Robinson, M. Berggren, R. Forchheimer, *Advanced Materials* **2005**, *17*, 353-358.
- [12] Q. Pei, G. Yu, C. Zhang, Y. Yang, A. J. Heeger, *Science* **1995**, *269*, 1086-1088.
- [13] J. H. Shin, N. D. Robinson, S. Xiao, L. Edman, *Advanced Functional Materials* **2007**, *17*, 1807-1813.
- [14] P. Andersson, D. Nilsson, P. O. Svensson, M. Chen, A. Malmström, T. Remonen, T. Kugler, M. Berggren, *Advanced Materials* **2002**, *14*, 1460-1464.
- [15] P. Tehrani, L. O. Hennerdal, A. L. Dyer, J. R. Reynolds, M. Berggren, *Journal of Materials Chemistry* **2009**, *19*, 1799-1802.
- [16] Z. M. Rittersma, *Sensors and Actuators, A: Physical* **2002**, *96*, 196-210.

- [17] D. Nilsson, T. Kugler, P. O. Svensson, M. Berggren, *Sensors and Actuators, B: Chemical* **2002**, 86, 193-197.
- [18] D. J. Macaya, M. Nikolou, S. Takamatsu, J. T. Mabeck, R. M. Owens, G. G. Malliaras, *Sensors and Actuators, B: Chemical* **2007**, 123, 374-378.
- [19] T. Lindfors, A. Ivaska, *Analytica Chimica Acta* **2001**, 437, 171-182.
- [20] J. Bobacka, A. Ivaska, A. Lewenstam, *Electroanalysis* **2003**, 15, 366-374.
- [21] M. Fahlman, W. R. Salaneck, *Surface Science* **2002**, 500, 904-922.
- [22] C. H. Hamann, A. Hamnett, W. Vielstich, *Electrochemistry*, Wiley, Weinheim, **1998**.
- [23] F. M. Gray, *Polymer Electrolytes*, The Royal Society of Chemistry, Cambridge, **1997**.
- [24] J. R. Macdonald, *Impedance Spectroscopy: Emphasizing Solid Materials and Systems*, Wiley, New York, **1987**.
- [25] S. M. Park, J. S. Yoo, *Analytical Chemistry* **2003**, 75, 455-461.
- [26] A. J. Bard, L. R. Faulkner, *Electrochemical Methods: Fundamentals and Applications*, Wiley, New York, **2001**.
- [27] J. Bisquert, *Electrochimica Acta* **2002**, 47, 2435-2449.
- [28] P. Colomban, *Proton Conductors*, Cambridge University Press, Cambridge, **1992**.
- [29] K. S. Cole, R. H. Cole, *Journal of Chemical Physics* **1941**, 9, 341-351.
- [30] P. Lorrain, D. R. Corson, *Electromagnetism: Principles and Applications*, Freeman, New York, **1997**.
- [31] P. Atkins, J. d. Paula, *Atkin's Physical Chemistry*, Oxford University Press, Oxford, **2006**.
- [32] F. Bordi, C. Cametti, R. H. Colby, *Journal of Physics Condensed Matter* **2004**, 16, 1423-1463.
- [33] A. Facchetti, M. H. Yoon, T. J. Marks, *Advanced Materials* **2005**, 17, 1705-1725.
- [34] J. Zaumseil, H. Sirringhaus, *Chemical Reviews* **2007**, 107, 1296-1323.
- [35] S. M. Sze, *Physics of Semiconductor Devices*, Wiley, New York, **1981**.
- [36] H. Sirringhaus, P. J. Brown, R. H. Friend, M. M. Nielsen, K. Bechgaard, B. M. W. Langeveld-Voss, A. J. H. Spiering, R. A. J. Janssen, E. W. Meijer, P. Herwig, D. M. De Leeuw, *Nature* **1999**, 401, 685-688.

- [37] R. J. Kline, M. D. McGehee, E. N. Kadnikova, J. Liu, J. M. J. Fréchet, *Advanced Materials* **2003**, *15*, 1519-1522.
- [38] J. F. Chang, B. Sun, D. W. Breiby, M. M. Nielsen, T. I. Sölling, M. Giles, I. McCulloch, H. Sirringhaus, *Chemistry of Materials* **2004**, *16*, 4772-4776.
- [39] L. A. Majewski, R. Schroeder, M. Grell, *Advanced Materials* **2005**, *17*, 192-196.
- [40] C. D. Dimitrakopoulos, S. Purushothaman, J. Kymissis, A. Callegari, J. M. Shaw, *Science* **1999**, *283*, 822-824.
- [41] M. Halik, H. Klauk, U. Zschieschang, G. Schmid, C. Dehm, M. Schütz, S. Malsch, F. Effenberger, M. Brunnbauer, F. Stellacci, *Nature* **2004**, *431*, 963-966.
- [42] L. A. Majewski, R. Schroeder, M. Grell, *Advanced Functional Materials* **2005**, *15*, 1017-1022.
- [43] H. G. O. Sandberg, T. G. Bäcklund, R. Österbacka, H. Stubb, *Advanced Materials* **2004**, *16*, 1112-1115.
- [44] T. G. Bäcklund, H. G. O. Sandberg, R. Österbacka, H. Stubb, *Applied Physics Letters* **2004**, *85*, 3887-3889.
- [45] A. S. Dhoot, J. D. Yuen, M. Heeney, I. McCulloch, D. Moses, A. J. Heeger, *Proceedings of the National Academy of Sciences of the United States of America* **2006**, *103*, 11834-11837.
- [46] M. J. Panzer, C. R. Newman, C. D. Frisbie, *Applied Physics Letters* **2005**, *86*, 1035031-1035033.
- [47] M. J. Panzer, C. D. Frisbie, *Journal of the American Chemical Society* **2005**, *127*, 6960-6961.
- [48] M. J. Panzer, C. D. Frisbie, *Journal of the American Chemical Society* **2007**, *129*, 6599-6607.
- [49] M. J. Panzer, C. D. Frisbie, *Advanced Materials* **2008**, *20*, 3176-3180.
- [50] L. G. Kaake, Y. Zou, M. J. Panzer, C. D. Frisbie, X. Y. Zhu, *Journal of the American Chemical Society* **2007**, *129*, 7824-7830.
- [51] J. D. Yuen, A. S. Dhoot, E. B. Namdas, N. E. Coates, M. Heeney, I. McCulloch, D. Moses, A. J. Heeger, *Journal of the American Chemical Society* **2007**, *129*, 14367-14371.
- [52] L. Herlogsson, X. Crispin, N. D. Robinson, M. Sandberg, O. J. Hagel, G. Gustafsson, M. Berggren, *Advanced Materials* **2007**, *19*, 97-101.

- [53] E. Said, X. Crispin, L. Herlogsson, S. Elhag, N. D. Robinson, M. Berggren, *Applied Physics Letters* **2006**, 89, 1435071-1435073.
- [54] L. Herlogsson, Y. Y. Noh, N. Zhao, X. Crispin, H. Siringhaus, M. Berggren, *Advanced Materials* **2008**, 20, 4708-4713.
- [55] Y. Sakai, Y. Sadaoka, M. Matsuguchi, *Sensors and Actuators, B: Chemical* **1996**, 35-36, 85-90.
- [56] Z. Chen, C. Lu, *Sensor Letters* **2005**, 3, 274-295.
- [57] Y. Li, M. J. Yang, Y. She, *Sensors and Actuators, B: Chemical* **2005**, 107, 252-257.
- [58] G. Casalbore-Miceli, A. Zanelli, A. W. Rinaldi, E. M. Giroto, M. J. Yang, Y. S. Chen, Y. Li, *Langmuir* **2005**, 21, 9704-9708.
- [59] G. Casalbore-Miceli, M. J. Yang, N. Camaioni, C. M. Mari, Y. Li, H. Sun, M. Ling, *Solid State Ionics* **2000**, 131, 311-321.
- [60] P. M. Harrey, B. J. Ramsey, P. S. A. Evans, D. J. Harrison, *Sensors and Actuators, B: Chemical* **2002**, 87, 226-232.
- [61] Y. Li, M. J. Yang, N. Camaioni, G. Casalbore-Miceli, *Sensors and Actuators, B: Chemical* **2001**, 77, 625-631.
- [62] K. G. Ong, C. A. Grimes, *Smart Materials and Structures* **2000**, 9, 421-428.
- [63] T. J. Harpster, B. Stark, K. Najafi, *Sensors and Actuators, A: Physical* **2002**, 95, 100-107.
- [64] J. B. Ong, Z. You, J. Mills-Beale, E. L. Tan, B. D. Pereles, K. G. Ong, *IEEE Sensors Journal* **2008**, 8, 2053-2058.
- [65] L. Herlogsson, M. Cölle, S. Tierney, X. Crispin, M. Berggren, *Advanced Materials* **2009**, In Press.
- [66] M. S. Gong, J. S. Park, M. H. Lee, H. W. Rhee, *Sensors and Actuators, B: Chemical* **2002**, 86, 160-167.
- [67] X. Lv, Y. Li, P. Li, M. Yang, *Sensors and Actuators, B: Chemical* **2009**, 135, 581-586.